ELSEVIER

Catalysis Today 53 (1999) 343–356

CATALYSIS TODAY

www.elsevier.com/locate/cattod

Nuclear magnetic resonance study of platinum catalysts containing alkali atoms

James A. Norcross[a,*,1], Charles P. Slichter[b], John H. Sinfelt[c]

[a] *Department of Physics and Materials Research Laboratory, University of Illinois, Urbana, IL, USA*
[b] *Department of Physics, Department of Chemistry and Materials Research Laboratory, 1110 West Green Street, University of Illinois, Urbana, IL 61801-3080, USA*
[c] *Exxon Research and Engineering, Annandale, NJ 08801, USA*

Abstract

We have used NMR to study the effects of adding alkali metals (Na, K, Rb, or Cs) to silica supported platinum clusters. Alkali metals are frequently added to metal catalysts, and to other catalysts as well, to serve as 'promoters'. We have also examined the effect of the alkali metals on adsorbed CO. The properties of the alkali metal itself were studied in samples containing Na. By performing a ^{23}Na–^{13}C double resonance with adsorbed CO, we determined that at least 26% of the sodium in the samples is on the platinum clusters. The ^{23}Na line shows no indication of a Knight shift and the ^{23}Na spin-lattice relaxation time varies as $1/T^2$, suggesting that the sodium orbitals mix with the platinum conduction band to a much lesser degree than do those of adsorbed CO. The NMR results lead us to conclude that the Na forms three-dimensional structures on the Pt, most likely small Na_2O clusters with sizes approaching molecular dimensions. We observed the effect of the alkali metals Na, K, Rb, and Cs on the NMR properties of adsorbed CO. In all cases the effects are small. The CO line is narrowed and shifted to higher frequency in the presence of the alkali metal while the CO spin lattice relaxation is slowed. The effect of the alkali metal is greater in the samples with the heavier alkali metals K, Rb and Cs. In the case of CO with Rb, for which the effect of the alkali metal is greatest, a modest change of about 10–15% in the parameters used to describe the NMR results is adequate to account for the effect of the Rb.

PACS: 76.60.-k; 82.65.Jv

1. Personal Prologue by C.P. Slichter

My interest in catalysis was sparked by a seminar John Sinfelt gave at the Chemistry Department of the University of Illinois over 20 years ago. Hearing him talk, I decided to see whether one could tackle some of the issues by means of nuclear magnetic resonance. Realizing the importance of being connected to someone with real expertise, I asked my close friend, Harry Drickamer (John's thesis advisor 'Doc') to see whether or not John would like to collaborate on such a venture. I was delighted when John said yes. Thus, began our university–industry collaboration: no contracts, no lawyers, or academic administrators, just two scientists with a common interest. And this is how John unwittingly became a professor, because all of our work has been as part of the Ph.D. Theses of my graduate students. We have studied supported catalysts of the second and third rows of the group VIII metals. Our first studies led to the discovery of the nuclear magnetic resonance of the surface layer of ^{195}Pt atoms. From there we progressed to study adsorbed

* Corresponding author.
[1] Present address. Magnetic Resonance Microsensors, Savoy, IL 61874, USA.

0920-5861/99/$ – see front matter
PII: S0920-5861(99)00129-7

molecules, their bonding, structure, and eventually reactions. In the process, John has helped educate 13 students, two post-docs, and me. Though the Exxon Research and Engineering Laboratory was 1000 miles from Champaign-Urbana, John was always ready for a phone call to seek his advice and guidance. My students called John directly, sometimes running up rather large phone bills. We talked with him about the general areas of greatest importance as well as the meaning of specific results. John was an active and interested participant in preparation of manuscripts describing the results. John's openness and warmth have won a special place for him in the regard of all of us, his students. What a successful teacher he has been!

2. Introduction

The action of a catalyst is frequently associated with a surface on which reactions may take place. Materials known as 'promoters' are often added to catalysts to improve their performance [1]. The presence of the promoter may alter the adsorptive properties of the catalytic surface and the way in which reactants dissociate or combine on the surface. The promoter can increase the rate of a reaction or change the selectivity of formation of a desired product. A promoter may also have a purely structural effect, e.g., increasing surface area or simply stabilizing the surface area of a catalyst during use.

In this paper, we describe a nuclear magnetic resonance (NMR) study of alkali atom promoters on supported Pt catalysts, including the situation in which CO is also adsorbed on the clusters. In the past decade, a large amount of the work seeking to clarify the action of promoters has been carried out using ultra-high vacuum (UHV) surface techniques [2–4]. The widespread use of alkali metal promoters in industrial catalysts has made them a frequent topic of these investigations. Alkali metal adsorption on transition or noble metal surfaces produces a localized lowering of the surface work function which varies with alkali metal coverage [5,6]. One explanation for the lowered work function is that electrons are transferred from the alkali metal to the surface. As the coverage increases, the extent of electron transfer from the alkali metal is reduced and there is a variation of the character of the adatoms from ionic to metallic. However, recent work has revealed that the electronic properties of alkali metal adatoms don't vary with coverage, suggesting that they are metallic at all coverages [7–9]. The presence of the alkali metal affects adsorbed CO molecules in several different ways. It reduces CO uptake and may block certain CO bonding sites, forcing CO to adsorb in sites of particular symmetry (i.e., linear or bridge sites) [10,11]. The thermal desorption spectroscopy (TDS) has revealed that CO molecules adsorbed on surfaces containing alkali metals adsorb preferentially on sites near to the alkali metal where they experience an increased binding energy with the surface [12–15]. Large downshifts in the C–O stretch frequency measured by high resolution electron energy loss spectroscopy (HREELS) indicate a lowering of the C–O bond strength [11,15–17]. This results in a lengthening of the C–O bond and an increase in CO dissociation [10,18].

CO bonds to transition metals via donation of electrons from its 5σ orbital to the conduction band of the metal accompanied by a concurrent back donation of electrons from the metal to the $2\pi^*$ antibonding CO orbital. Addition of K to the metal surface lowers the work function of the metal and is thought to lower the antibonding levels of adsorbing CO molecules making possible a greater back donation. A metastable quenching spectroscopy (MQS) study of CO and K on Ni (111) has shown directly the enhancement of $2\pi^*$ backdonation [10]. However, the strength of the K–CO interaction, as evidenced by lower bond symmetry, larger adsorption energies and much weaker C–O bonds indicates that a simple enhancement of $2\pi^*$ backbonding cannot be the sole cause of all the effects seen in these systems.

There are three basic models for an additional interaction between K and CO. Weimer proposes that adsorbing CO molecules rehybridize from a metallic sp character to an organic sp^2 character allowing for an increase in CO bond coordination and greater overlap between CO $2\pi^*$ orbitals and metal d bands [19,20]. Formation of K and CO complexes is an explanation advanced by Lackey et. al. to explain the presence of coincident K and CO desorption peaks in their TDS study [21]. A direct interaction consisting of charge transfer from the CO 1π to neutralize an ionic K adatom is used by Heskett to explain a measured reduction in CO symmetry and shifts in the CO 1π and K 3π levels [17].

Although the studies to date seeking to elucidate the promoter action of alkali metals in a non-oxidic state using high vacuum techniques have been of interest for surface science, one must remember that the alkali metal is commonly present as an oxide in industrial catalysts. A classic example is the promoted iron catalyst used in ammonia synthesis, where the promoter is K_2O [1]. Indeed, a major goal of our study is determination of the state of the alkali atoms. Are they in oxides, as in the ammonia synthesis case, or are they more like the alkali metals studied by ultra high vacuum, or does neither description work? We find that the magnetic resonance evidence favors the oxide model.

Nuclear magnetic resonance (NMR) is one method that has been used successfully to study actual catalyst surfaces [22]. The usefulness of NMR as a surface probe arises from its ability to explore the local magnetic fields experienced by nuclei both on and in the surface. In this paper we report the results of our NMR study of CO adsorbed on silica supported platinum clusters in the presence of alkali metals. The alkali metals are typical of the promoters in a number of industrial catalysts. This work had two principal goals; (i) to determine the properties of the alkali metal in the samples and (ii) to study the effect of the alkali metal on the properties of adsorbed CO.

The properties of the alkali metal were determined by observing the NMR of the alkali metal ^{23}Na, as well as that of ^{195}Pt in the surface and ^{13}C in adsorbed CO. By performing a ^{23}Na–^{13}C double resonance experiment with adsorbed ^{13}CO we verified that a substantial amount of the Na in the sample is on the platinum clusters. The ^{23}Na line position indicates that the sodium in the samples is ionic in nature. This fact, together with the results of measurements of the ^{23}Na spin–lattice relaxation and ^{195}Pt lineshape, lead us to conclude that the sodium exists as an ionic compound, most likely Na_2O, which interacts with the metal surface to a much lesser degree than does adsorbed CO.

We studied the effect of the alkali metal on adsorbed CO by observing the ^{13}C NMR of CO in samples with and without alkali metals. We measured the lineshape and relaxation of ^{13}CO with the alkali metals Na, K, Rb and Cs. The presence of the alkali metals has a small, yet measurable, effect on the lineshape and relaxation, with the heavier alkali metal additives producing greater changes in the properties of the CO. The fact that the alkali metals in the samples exist as oxides limits the effect they have on the CO.

3. Experimental details

The samples were prepared in the laboratories of the Exxon Research and Engineering Company by a standard method of impregnation. A silica (SiO_2) powder with surface area $\sim$700 m^2/g was wet with a chloroplatinic acid solution. The concentration of the acid was adjusted to give final samples which were 5% platinum by weight. The resulting material was then dried at 383 K and finally exposed to hydrogen at 723 K. This yielded platinum clusters about 30 Å in diameter supported on the silica substrate. The clusters are assumed to be cubo–octahedra, consisting primarily of (111) faces with about 5 atoms on a face edge. The dispersion of the Pt, which is the ratio of surface atoms to total atoms in a cluster, was around 35% as determined by hydrogen chemisorption. The surface area of the platinum was about 4 m^2/g of sample. Alkali metals (Na, K, Rb, Cs) were added to the catalyst by wetting it with an alkali metal hydroxide solution. The catalyst was again dried and exposed to hydrogen at elevated temperatures. The alkali metal loading in the sample was set to give a ratio of alkali metal atoms to surface Pt atoms of 0.66.

After the samples were received, they were cleaned to remove molecules adsorbed on the metal surface during its exposure to the atmosphere. First the samples were heated to 573 K and evacuated to 10^{-6} Torr. Next they were exposed to alternating flows of ultra-pure H_2 and O_2 to chemically remove any remaining adsorbates. The metal was then reduced with a final H_2 flow and the sample re-evacuated and cooled. CO gas, isotopically enriched to 99% in ^{13}C, was adsorbed on the metal surface at room temperature. The sample was exposed to the gas at low pressure over a period of 15 min in order to reduce heating of the surface produced by the exothermic adsorption. The total gas exposure was adequate to provide a full coverage on the metal clusters with a small overpressure. After adsorption of the gas, the system was evacuated to remove any molecules physisorbed on the support and the samples were sealed under vacuum in quartz tubes. The samples are labeled by catalyst metal, alkali metal additive

and adsorbate. Pt–Na–CO is a sample with platinum clusters, Na additive and adsorbed CO.

All of the measurements reported here were made in a magnetic field of about 8.2 Tesla. To take advantage of the increased signal to noise ratio at low temperatures, measurements were made at 77 K with the sample in liquid nitrogen, unless indicated otherwise.

The NMR methods used to investigate the promoted samples were those previously employed by the Slichter group to study catalysts. They are described in a review work by Ansermet et al. [23].

4. Results

4.1. Properties of the alkali atoms

During the course of this work, platinum catalysts containing the alkali metals Na, K, Rb and Cs were studied. To determine the characteristics of the alkali metal in the samples, the NMR properties of the platinum clusters and adsorbed CO were investigated as well as those of the alkali metal itself. The relatively small number of nuclei in the sample made NMR measurements of adsorbed nuclei difficult. For this reason the alkali metal studied was ^{23}Na, since its large gyromagnetic ratio and 100% natural abundance increased the signal that could be detected from a fixed number of nuclei.

4.1.1. Charge character of alkali atoms

There are several factors which may influence the resonance frequency of ^{23}Na in the catalyst samples. If Na atoms form chemical bonds with the surface or adsorbates they exhibit a chemical shift. Normal ^{23}Na chemical shifts are of the order of 10–20 ppm [24]. The ^{23}Na might also develop a Knight shift via the mixing of its orbitals with the conduction band of the metal surface. For CO on Pt, the adsorbed CO develops a 130 ppm Knight shift. The Knight shift incurred in this way is given by

$$K_s = \frac{8\pi}{3} |\Psi_a(0)|^2 \chi_s^m \alpha. \quad (1)$$

where Ψ_a (0) is the value of the adsorbate wave function at the position of the nucleus, χ_s^m is the spin susceptibility of the metal (0.95 for Na [25], 22.9 for Pt [26], both in 10^{-6} cgs volume units) and α is the mixing fraction. For a Na atom in bulk Na metal, $\alpha = 1$ and K_s is 1120 ppm [27] For Na on Pt the Knight shift may be estimated to be

$$K_s(\text{Na on Pt}) \approx K_s(\text{Na metal}) \frac{\chi_s^{Pt}}{\chi_s^{Na}} \alpha = (27,239\,\text{ppm})\alpha. \quad (2)$$

Even for an α as small as 1%, the Knight shift of ^{23}Na on Pt could be as large as 300 ppm.

In addition to the magnetic effects, spin 3/2 ^{23}Na also experiences electric quadrupole effects which can result in extensive line broadening and the development of discrete quadrupole satellite lines. The value of the Na quadrupole coupling constant in general can be as large as 2 MHz [28].

Fig. 1 shows the ^{23}Na spectrum for the sample Pt–Na obtained by integrating spin echoes at different frequencies over a 3 MHz range. The reference compound for the Na frequencies is a NaOH solution. The spectrum shows a single resolved feature at a position near 0 frequency. A lineshape of the Na feature obtained from the Fourier transform of a spin echo at 0 frequency is shown in Fig. 2a. The Na line is asymmetric, favoring lower frequencies and is similar in shape to the Na lines for samples of Na_2O and Na_2CO_3 (Fig. 2 b and c). The characteristics of the ^{23}Na lines for the three samples are summarized in Table 1 The Na line in Pt–Na is at a frequency typical of the chemical shift of ionic Na compounds and shows no sign of a

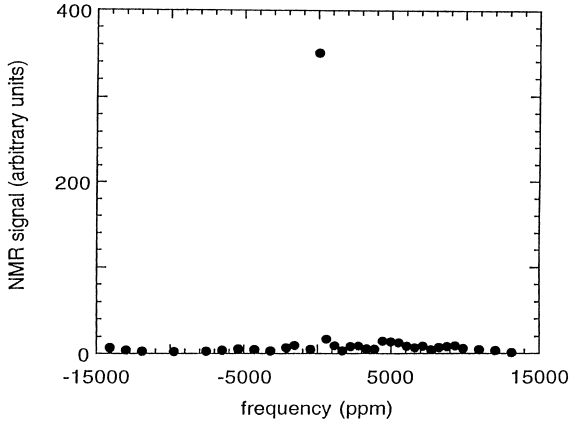

Fig. 1. Spectrum of the sample Pt–Na-clean over a 3 MHz range about the frequency of Na in NaOH.

Table 1
Properties of the ^{23}Na line for various samples. The reference compound was a NaOH solution

Sample	Peak position	First moment (ppm)	Full width at half max (ppm)
Pt–Na-clean	−9.0	−30.2	143
Na_2O	−9.0	−22.3	112
Na_2CO_3	12.2	−8.9	77

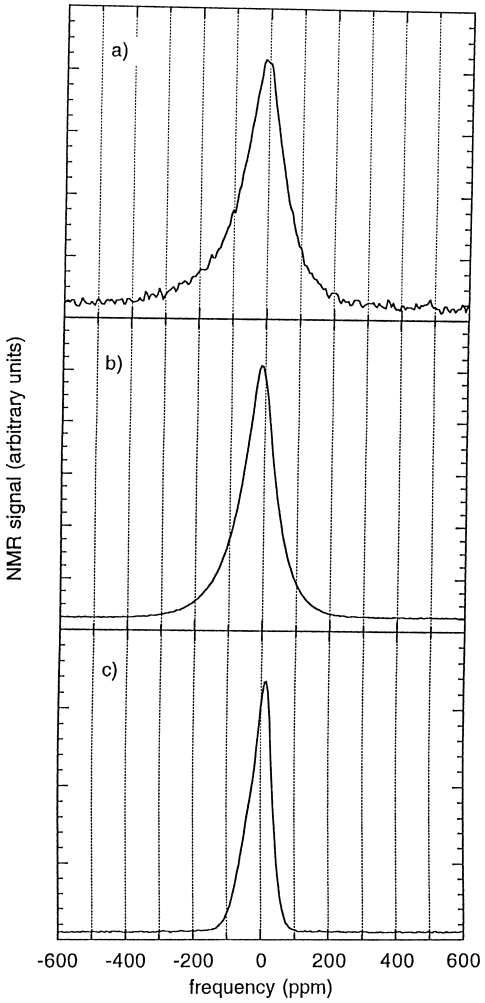

Fig. 2. ^{23}Na lineshapes for (a) Pt–Na-clean, (b) Na_2O, and (c) Na_2CO_3. (Fourier transform of second-half of the spin echo).

Knight shift indicating that the Na in Pt–Na is ionic in character. Since K, Rb and Cs have lower ionization potentials than Na, we assume that they also have ionic character in our samples.

To determine whether the observed ^{23}Na resonance accounted for all the sodium in the sample, a calibration of the signal from this resonance with that from a known amount of Na was performed. The calibration sample was a NaCl solution. First an H_1 calibration measurement was made to determine whether the ^{23}Na resonance for Pt–Na corresponded to all the Na quadrupole transitions or just the $(+1/2)\leftrightarrow(-1/2)$ 'central' transition. In pulsed NMR of quadrupolar nuclei, both signal intensity and pulse length depend on whether all or only some of the quadrupole transitions are being flipped [29]. For the spin 3/2 ^{23}Na, the pulse length required to flip only the central transition is one half that required to flip all the quadrupole transitions. In the NaCl calibration sample, motion of the Na^+ ions results in an averaging of quadrupolar interactions and the resonance for this sample represents all the ^{23}Na quadrupole transitions. The pulse length measured for Pt–Na is half that measured for the calibration sample, indicating that the resonance observed for Pt–Na represents only the ^{23}Na central transition. The Na signal calibration was concluded by comparing the signal amplitude from Pt–Na with that from the calibration sample. When corrected for relaxation effects and normalized to account for differing number of nuclei in the samples the ratio of the signal from Pt–Na to that of the calibration sample is 0.20 ± 0.02. This number is exactly that fraction of intensity obtainable in a pulse experiment which flips only the central transition of a spin 3/2 nuclear species [29] making it clear that the observed ^{23}Na resonance accounts very well for all the Na in Pt–Na.

The ^{23}Na central transition experiences a second order electric quadrupole shift. However, even for a value of e^2qQ/h of 2 MHz, the second order quadrupole shift for ^{23}Na in an 8.2 Tesla field would be only 20 ppm. In addition, the ^{23}Na resonance may also have a chemical shift of as much as 20 ppm. Thus, the sodium in Pt–Na could have a Knight shift of order 40 ppm that is concealed by offsetting second order quadrupole and chemical shifts. To develop such a Knight shift, the fraction α describing the mixing of the Na wavefunc-

tion with the metal conduction band would need to be only 0.0015 (Eq. (2)).

4.1.2. Location of alkali atoms

The method used to add the alkali metals to the samples in this work allows the alkali metal to reside either on the metal clusters or on the silica support. In order to determine what portion of the alkali metal was on the surface of the platinum clusters a ^{23}Na–^{13}C SEDOR experiment was performed on the sample Pt–Na–CO. Destruction of the ^{23}Na signal produced by flipping ^{13}C indicates that a substantial amount of the sodium is on the platinum clusters.

Spins which are subject to magnetic fields that vary during the period in which an echo is being formed experience irreversible dephasing which results in a reduction of the echo amplitude. The dipolar field created by neighboring spins which are flipped during the formation of the echo is an important time varying field source. The z component of the dipole field experienced by a spin I_1 due to a neighboring spin I_2 is

$$H_{\mathrm{d}}^{z} = \frac{\gamma_2 \hbar}{r^3} m_2 (3\cos^2\theta - 1) \tag{3}$$

where m_2 is the z component of I_2. Spins I_1 with neighbors spin up precess more rapidly than those with neighbors spin down. If during the formation of an I_1 spin echo the neighboring spins are flipped, the difference in precession rate for each I_1 before and after the flip will produce a reduction in the I_1 echo amplitude. If the I_2 spins are flipped at a time t after the initial I_1 pulse, the amplitude of the echo is modulated as

$$M(t) = M_0 \cos(\gamma_1 H_{\mathrm{d}}^{\mathrm{total}}\, t) \tag{4}$$

where $H_{\mathrm{d}}^{\mathrm{total}}$ is the sum of the dipole fields of all the neighboring I_2 spins. A powder average of the $(3\cos^2\theta - 1)$ term in H_{d}^{z} produces a decaying cosine oscillation. When I_1 and I_2 are like spins, as for neighboring ^{13}C atoms in adsorbed CO, the neighbors are flipped by the pulse which produces the echo causing a decay in the echo amplitude commonly known as the 'slowbeat.' For the case in which the neighboring spins are unlike spins, the echo modulation can be produced by performing a double resonance experiment. Fig. 3 shows the spin echo double resonance (SEDOR) pulse sequence. The experiment consists of

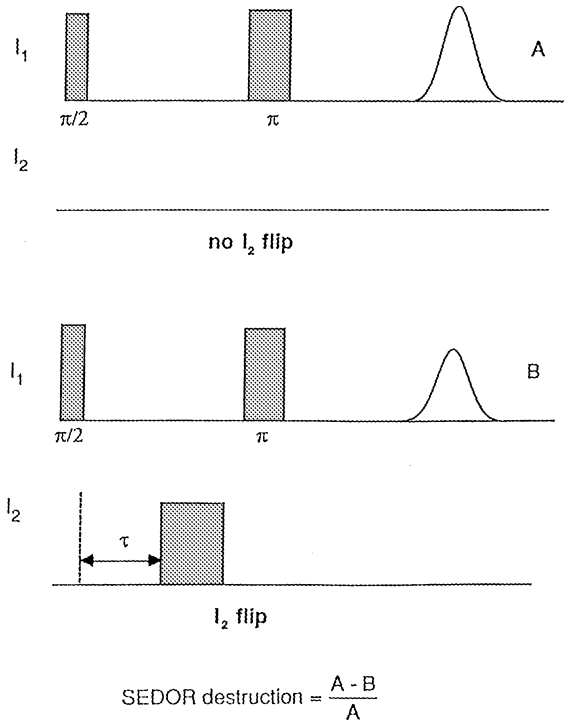

Fig. 3. SEDOR pulse sequence

two parts. In the first an I_1 spin echo is formed with a normal two-pulse sequence. Next, the same two-pulse sequence is applied to I_1, but at a time t after the initial I_1 pulse a π pulse is applied to I_2 reducing the I_1 echo amplitude. The result of the experiment is expressed as the fractional destruction of the I_1 echo amplitude as a function of t and has the form

$$\text{SEDOR destruction} = 1 - \cos(\gamma_1 H_{\mathrm{d}}^{\mathrm{total}} t) \tag{5}$$

The ^{23}Na–^{13}C SEDOR experiment consisted of observing the effect on the ^{23}Na signal of flipping the ^{13}C in adsorbed CO. The CO line for the sample had the 130 ppm Knight shift representative of CO on the platinum clusters. Fig. 4 shows the fractional destruction of the ^{23}Na spin echo amplitude as a function of t. The non-zero destruction of the ^{23}Na signal produced by the carbon flip indicates that at least some of the sodium is on the metal clusters near CO. The surface area of the platinum clusters in the samples is about 4 m^2/g while that of the support is nearly 700 m^2/g. If the Na went indiscriminately on the clusters and support, the destruction would be expected to rise to a maximum of less than 1%. The fact that the

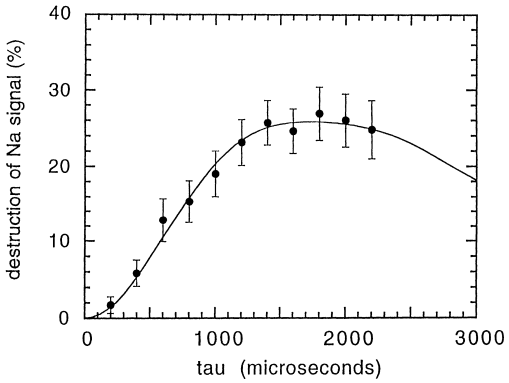

Fig. 4. Destruction of the ^{23}Na signal for Pt–Na–CO by SEDOR between ^{23}Na and adsorbed ^{13}CO. The curve shown is the calculated destruction for Na with a single CO neighbor.

destruction rises to nearly 26% indicates that the Na prefers to be on the metal clusters, suggesting a larger Na binding energy on the platinum than on the silica support. The fact that the destruction of the ^{23}Na signal is not complete could indicate either that part of the sodium is on the support or that the sodium forms extended structures on the platinum surface. The Na in such structures which is sufficiently far from CO, would not be affected by the ^{13}C flip.

In analysis of the destruction curve, models are considered in which the Na has from one to four CO neighbors which are symmetrically arranged about it. In the models, no consideration is given to the underlying structure of the Pt surface (i.e., the Na and CO are not constrained to bond in sites of high symmetry). Fig. 4 shows the calculated SEDOR curve for the destruction produced by the dipolar interaction (Eq. (5)) between ^{23}Na and ^{13}C for the case of a single CO neighbor. The Na–C distance and fraction of sodium with CO neighbors for each model are shown in Table 2. There are two conclusions that can be drawn from this simple analysis. The first is that the peak of the destruction curve puts a lower limit of about 26% on the fraction of Na that is on the Pt. Using this fraction and the known Na loading, the Na coverage should be at least 0.17. From Table 2 it is evident that if the Na has an even number of symmetrically placed neighbors, the fraction of sodium on the platinum could be larger still. The reason for this is that Na's with equal numbers of spin up and spin down neighbors are unaffected by the ^{13}C flip. It also seems that the Na and CO are no closer together than about 2.7 Å. This is approximately the distance between similar bonding sites on adjacent Pt atoms.

Table 2
Parameters of SEDOR fits for Na with symmetrically arranged CO neighbors

No. neighbors	Na–C distance (Å)	Fraction of Na with CO neighbors
1	2.9	0.22
2	3.7	0.43
3	3.6	0.23
4	2.7	0.30

4.1.3. Structure of the alkali metal on the clusters

There are two possible extended structures the alkali metal can form on the platinum clusters. One is a two-dimensional island and the other is a three-dimensional cluster. The product of the alkali metal loading and the Na–C SEDOR destruction indicates that the Na coverage in our samples could be as large as 0.17. A monolayer of K on Pt (111) is only 0.30 [5,6]. This implies that if the sodium spreads out in two-dimensional structures, there could be as much as half a monolayer on the surface of the platinum clusters.

The possibility that there is near a monolayer of alkali metal on the samples is refuted by two experimental results. The first of these is that the ^{13}CO spin echo amplitude, which is a measure of the number of CO molecules in the sample, when properly corrected for relaxation effects and dispersion is nearly the same on samples with and without alkali metals. In single crystal studies, the sticking coefficient of CO, which is a measure of the amount of CO adsorbed on the surface for a given exposure of gas, decreases with increasing alkali metal coverage. That the CO might adsorb on top of the alkali metal, contrary to the result of UHV studies, is discounted by the fact that the CO line in the promoted samples has the 130 ppm Knight shift characteristic of CO on platinum.

The second result which denies the possibility of near monolayer alkali metal coverages is that, as we show below, the CO density is lower on the samples which contain alkali metals than on samples which do not. This eliminates the possibility that the alkali metal forms islands of some extent with the full coverage of CO adsorbing in compacted patterns on the clean

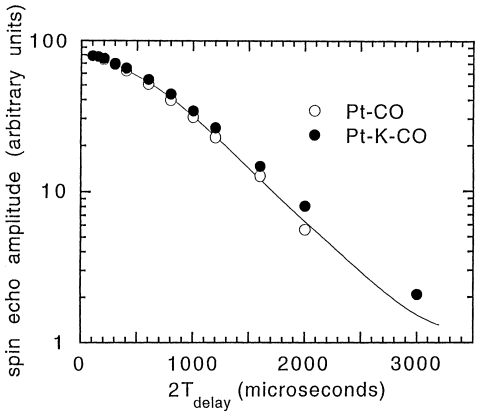

Fig. 5. ^{13}C spin–spin relaxation for Pt–CO and Pt–K–CO. The solid curve is a calculation of the relaxation for CO in a c(4 × 2) pattern on Pt(111).

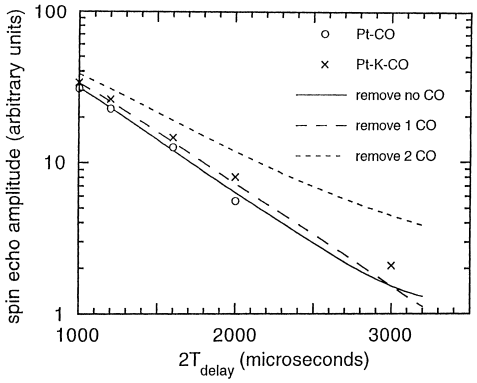

Fig. 6. Calculations of spin–spin relaxation for CO in a c(4 × 2) pattern with from 0 to 2 CO's removed.

surface. Fig. 5 shows the spin–spin relaxation curve for the sample Pt–CO (echo amplitude versus time at which the echo occurs). Ansermet et al. were able to fit the spin–spin relaxation for CO on Pt using a powder average of the dipolar coupling (Eq. (3)) between CO's adsorbed in a c(4 × 2) pattern on Pt (111) and a spin–spin relaxation time, T_2, of 2.8 ms [30]. A calculation of the relaxation with the same $c(4 \times 2)$ pattern and exponential is also shown in Fig. 5. The figure also shows a comparison of the spin–spin relaxation curves for the samples Pt–CO and Pt–K–CO. If the CO on the promoted samples formed compacted structures with a greater density, the $1/r^3$ term in the dipolar coupling which determines the initial decay would cause the spin–spin relaxation curve to fall more rapidly. Contrary to this result, in each of the samples containing alkali metals, the ^{13}C spin–spin relaxation decays more slowly than it does for the sample without the alkali metal. The slower decay indicates a lower CO density on the alkali metal containing samples. Fig. 6 shows a calculation of the spin–spin relaxation for the case in which the CO density is lowered by removing one or two out of every nine CO's. Less than two out of every nine CO molecules need to be removed in order to reduce the density enough to yield the observed relaxation. It is obvious that the CO density changes very little in the presence of the alkali metal.

We have then a picture of our samples in which there is a large amount of alkali metal on the clusters and yet there is little reduction in the amount of CO adsorbed and the CO density is only slightly smaller. The SEDOR result indicates that the CO and Na are not closer together than about 3 Å. The only way that this can be is if the alkali metal forms three dimensional structures that extend above the metal surface. The similarity between the ^{23}Na lineshape for Pt–Na (Fig. 2a) and that for Na_2O (Fig. 2b) suggests that Na_2O clusters (possibly with sizes approaching molecules in dimensions) are likely structures. The base of the structures must be restricted so as to not limit CO adsorption.

4.1.4. Interaction of alkali metal with platinum surface

CO bonds to a metal surface through mixture of its valence electrons with the metal conduction band. The result of this method of bonding is evident in several of the magnetic resonance properties of the CO-metal system. One is the 130 ppm Knight shift developed by the CO. Another is the variation of the CO T_1 with temperature according to the expression T_1T = constant as determined by both Ansermet [31] and Durand [32]. A Knight shift and T_1T = constant behavior are both characteristics of a metal. The bond formed when the CO adsorbs on the metal surface causes the CO to become metallic in nature. In addition to these changes in the property of the CO upon adsorption, the metal surface peak is shifted in frequency due to a change in the surface density of states caused by the chemisorption bond. It has already been demonstrated that the alkali metal in a given sample shows no sign of having a Knight shift. To further

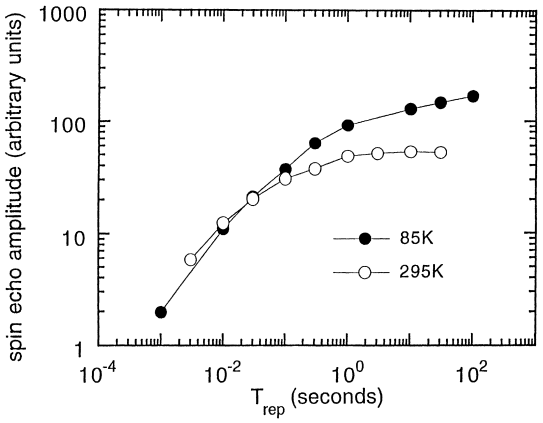

Fig. 7. ^{23}Na spin–lattice relaxation for Pt–Na-clean at 85 and 295 K.

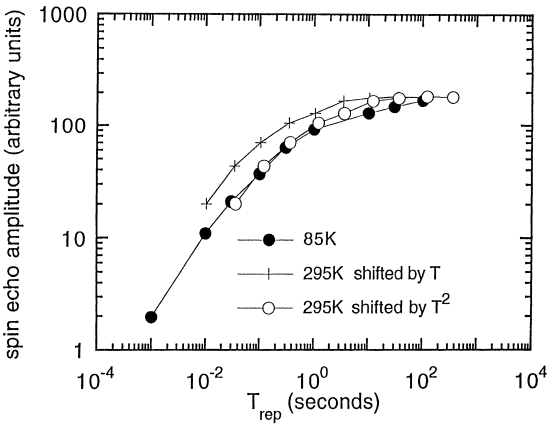

Fig. 8. ^{23}Na spin–lattice relaxation for Pt–Na-clean at 85 and 295 K. The 295 K curve has been scaled in amplitude by a Boltzman factor and shifted in time by factors of T and T^2.

examine the interaction between the alkali metal and the Pt surface the ^{23}Na spin–lattice relaxation and the 195 Pt surface peak were investigated.

Fig. 7 shows the ^{23}Na spin–lattice relaxation curves measured by progressive saturation for Pt–Na at 85 K and 295 K. The curves are slowly varying, indicating a distribution in relaxation rates. This result is not surprising since the spin 3/2 Na can undergo relaxation by magnetic dipole or electric quadrupole mechanisms. In addition, the relaxation of adsorbates may depend on bonding site as has been determined for CO on Pt by Ansermet et al. [31] Durand has shown for CO on Pt, however, that despite the distributed behavior of the relaxation, it is possible to scale the curves at various temperatures to determine the temperature dependence of the relaxation [32]. The scaling consists of weighting the amplitude of the signal by a Boltzman factor to account for the difference in the equilibrium magnetization at different temperatures, together with a time scale shift to represent the effect of temperature on relaxation. Fig. 8 shows the result of scaling the relaxation curve for Pt–Na at 295 K in this fashion with time scale shifts of T and T^2. It is clear that the relaxation does not vary as $1/T$ but instead as $1/T^2$. The $1/T^2$ behavior of the relaxation is typical of nuclei relaxing by electric quadrupole processes.

Earlier, it was concluded that although the Na line showed no indication of a Knight shift, there could be a Knight shift of order 40 ppm concealed by offsetting chemical and quadrupole shifts. Korringa has shown that the interaction with conduction electrons which produces the Knight shift also gives rise to spin–lattice relaxation which for Na is given by the expression [33].

$$T_1 T K^2 = 3.76 \times 10^{-6}(\mathrm{sK}) \quad (6)$$

For Na with a Knight shift of less than 40 ppm at 77 K this would yield a conduction electron contribution to T_1 of more than 31 s. This value is too long to compete with the quadrupolar relaxation which we observe.

The platinum lineshape of sample Pt(34)–Na is shown in Fig. 9. (The (34) indicates that the dispersion of the Pt is 34% as determined by H_2 chemisorption. The dispersion measurements have an uncertainty of

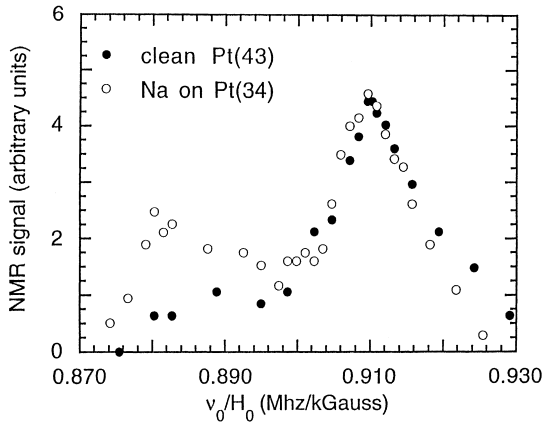

Fig. 9. ^{195}Pt lineshapes for Pt–Na-clean and Pt-clean. The curves are scaled to have equal area in the surface peak near $\nu_0/H_0 = 0.910$ MHz/kG.

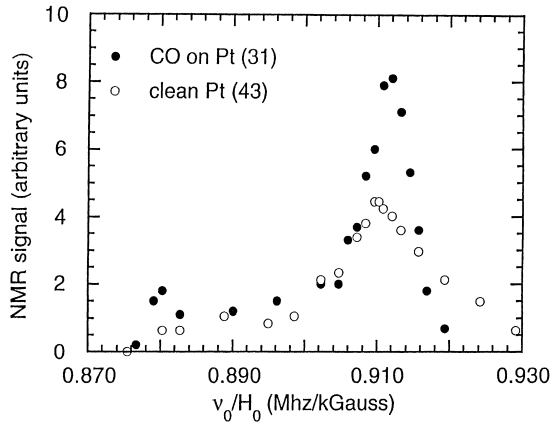

Fig. 10. ^{195}Pt lineshapes for Pt–CO and Pt-clean. The curves are scaled to have equal area in the surface peak at $\nu_0/H_0 = 0.910$ MHz/kG.

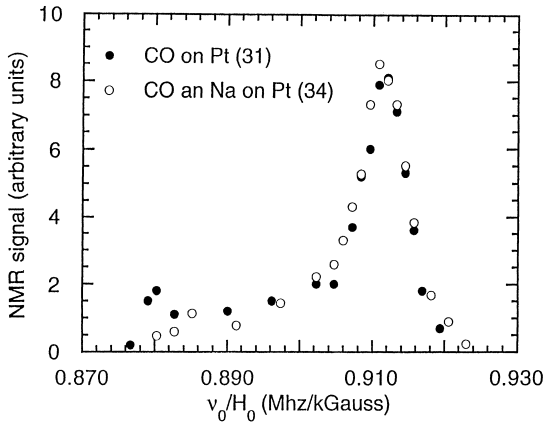

Fig. 11. ^{195}Pt lineshapes for Pt–CO and Pt–Na–CO. The curves are scaled to have equal area in the surface peak at $\nu_0/H_0 = 0.910$ MHz/kG.

about 10% of the value.) The platinum line is extremely broad, extending over a range of frequencies of almost 6%. The three mechanisms which broaden the line are a variation of the susceptibility of the platinum clusters with cluster size, chemical and Knight shift anisotropies, and a difference in the electronic environment experienced by platinum nuclei in different layers of a given cluster. There are two distinct features on the line. The first, at ν_0/H_0 of about 0.910 MHz/kG, is associated with platinum in and near the surface. The second, at 0.880 MHz/kG, has the −3.4% Knight shift typical of platinum metal and corresponds to platinum nuclei in the interior of the clusters. The intensity between the two features arises from nuclei in environments which are between that of the bulk and the surface. The ν_0/H_0 of the surface peak is near to that of H_2PtI_6 (0.9094 MHz/kG), the common reference compound for determining platinum chemical shifts.

H.E. Rhodes et al. have determined that the presence of adsorbates on the surface shifts the ^{195}Pt surface peak with respect to the surface peak for clean Pt [34]. The shifted peak falls within the range of typical ^{195}Pt chemical shifts which vary from −1500 to 12,000 ppm [35] They claim that the position and shape of the surface peak vary with the type of adsorbed molecule and hence provide a 'fingerprint' which can identify the adsorbed molecules. Fig. 10 shows the effect on the platinum surface peak of the mixing of adsorbate orbitals with the surface conduction band for the case of the adsorption of CO. The curves for Pt(31)–CO and Pt(43) are scaled to have equal areas under the surface peak. The 195 Pt surface peak in the presence of the CO is narrowed and shifted to higher frequency. Fig. 9 shows a comparison of the lineshape for a clean platinum surface Pt(43) with that for the sample Pt(34)–Na. The presence of the sodium has a much smaller effect on the platinum surface peak than does CO. This may be in part due to the fact that the CO coverage is 0.5 while the Na coverage is only 0.17. There is a great deal more intensity at the bulk position for the sample of Na on Pt due to a difference in the dispersion of the samples. Fig. 11 shows the ^{195}Pt lineshape for Pt(31)–CO and for Pt(35)–Na–CO. Once again, the presence of the Na seems to have little noticeable effect on the surface peak. The fact that the presence of the alkali metal has little effect on the ^{195}Pt surface peak suggests that it forms a weak bond to the platinum surface.

4.2. Effect of alkali metal on properties of adsorbed CO

After having determined that at least a portion of the alkali metal in the samples was on the metal clusters, the next goal was to determine what effect the presence of the alkali metal had on adsorbed CO. CO adsorption on Pt clusters has been studied extensively using NMR [30–32,36].

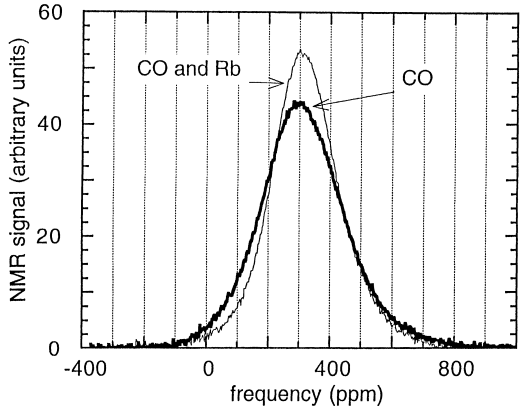

Fig. 12. ^{13}C lineshapes for Pt(31)–CO and Pt(35)–Rb–CO. The curves are scaled to have equal area.

The lineshape for CO in the sample Pt(31)–CO is shown in Fig. 12. The line is shifted up in frequency by about 300 ppm relative to the frequency of ^{13}C in tetramethylsilane (TMS) which is the common reference for expressing ^{13}C shifts. This shift arises from two different sources. The first is a chemical shift caused by the bonding of the CO to the platinum. The chemical shift for platinum carbonyls ranges from 165 ppm for linearly bonded carbons to 225 ppm for bridge bonded carbons [37]. CO bonds in linear sites on Pt(100) and in both linear and bridge sites on Pt(111). The other shift component is a Knight shift produced by mixing of the CO molecular orbitals with the conduction band of the Pt surface. The ^{13}C line is also broadened in the catalyst samples. There are three major sources of CO line broadening. Since the chemical and Knight shifts are describable by anisotropic second rank tensors, a powder sample experiences a broadening of the CO line due to chemical and Knight shift anisotropies. The third source of CO line broadening is the additional inhomogeneous field created by the magnetic susceptibility of the Pt clusters which has a magnitude of about 100 ppm.

In order to investigate the effect of alkali metals on the CO lineshape, the ^{13}C lineshapes for CO on samples with the alkali metals Na, K, Rb and Cs were measured. Fig. 12 shows a comparison between the CO lineshapes for the samples Pt(31)–CO and Pt(35)–Rb–CO. The lines are scaled to have equal areas. The presence of the Rb narrows the CO line and shifts it to slightly higher frequency. The other alkali metals affected the CO line in a similar manner, but to a lesser degree. A summary of the ^{13}C lineshape results is recorded in Table 3. The changes in position and width of the CO line are greater for samples containing the heavier alkali metals Rb and Cs. However, the effect of any of the alkali metals is small, with the greatest narrowing being only 12% and the largest shift being just 7 ppm for the 300 ppm broad line.

Table 3
Properties of the CO line in various samples

CO with	First moment (ppm)	Root second moment (ppm)
No alkali	313.8	144.3
Na	313.6	138.1
K	314.7	131.0
Rb	320.6	127.0
Cs	320.6	135.3

The final characteristic of the adsorbed CO that was investigated was its spin–lattice relaxation. The spin–lattice relaxation at 77 K for CO on highly dispersed Pt samples like ours has been studied extensively by J.P. Ansermet [31]. Ansermet determined that the CO spin–lattice relaxation could be described by the sum of four exponentials with relaxation times of 6 and 1.3 s, 300 and 9 ms. He measured the spin–lattice relaxation for a number of samples of various dispersions and CO coverages. Using these measurements and single crystal results concerning the binding energies and adsorption sites on the (111) and (100) faces he was able to assign the times of 6 s, 300 ms and 1.3 s to the relaxation occurring at linear and bridge sites on the (111) face and linear sites on the (100) face, respectively.

Fig. 13 shows the spin–lattice relaxation curve for the sample Pt–CO measured by progressive saturation. An attempt to fit the relaxation curve with the four relaxation times determined by Ansermet did not result in a good fit. This may be a result of a support effect, since our samples have a SiO_2 support while those of Ansermet had an Al_2O_3 support. A good fit of the relaxation curve for Pt–CO was obtained with three components with relaxation times of 1.09 s, 133 and 4 ms which are similar to the three shorter relaxation times of Ansermet. The fraction of each component is shown in Table 4and the resultant fit is also shown in Fig. 13.

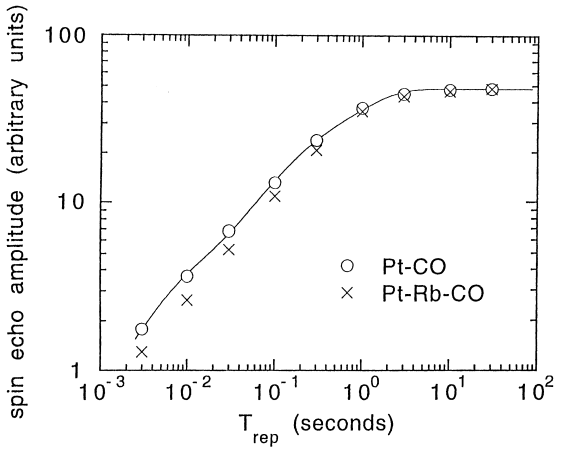

Fig. 13. ^{13}C spin–lattice relaxation for Pt–CO and Pt–Rb–CO. The solid curve is a fit of the relaxation for Pt–CO calculated using three exponentials with relaxation times 1.09 s, 133 and 4 ms.

Table 4
Amplitudes of the three exponentials used to fit CO spin–lattice relaxation

Relaxation time	CO with				
	No alkali	Na	K	Rb	Cs
1.09 s	0.62	0.67	0.71	0.72	0.66
130 ms	0.32	0.28	0.25	0.25	0.30
4 ms	0.06	0.05	0.04	0.03	0.04

To determine the effect of the alkali metal on the CO relaxation, the ^{13}C spin–lattice relaxation was measured for samples with Na, K, Rb, and Cs. The spin lattice relaxation curve for Pt–Rb–CO, Fig. 13, shows that the CO relaxes more slowly in the presence of the Rb. The CO relaxation is also slowed with the other alkali metals. Once again, as was the case with the lineshape, the effect of the alkali metal is smallest in the case of Na while it is greatest with K or Rb. In order to get an idea of the extent to which the relaxation is slowed, the relaxation curves for the samples containing the alkali metals were fit with the same three relaxation times used to fit the curve for Pt–CO by allowing the amplitudes of the exponentials to vary. In this way good fits were obtained for the relaxation for each sample with an alkali metal additive. The results of the fits are shown in Table 4. As can be seen, for the case of CO with Rb in which the effect on the spin–lattice relaxation is the largest, a modest change in the amplitudes of the two longest relaxation components by about 10–20% is able to describe the slower relaxation.

5. Conclusions

In this paper we have reported the results of our NMR study of platinum catalysts containing alkali metals. One of the important conclusions of our work is that a large amount of the alkali metal in our samples is on the platinum clusters. Our SEDOR results indicate that at least 26% of the sodium in the sample Pt–Na is on the platinum surface. This number is approximately 40 times larger than would be expected if the sodium went on the support and the platinum clusters to an extent which was determined by their relative surface areas. With such a large fraction of the sodium on the platinum, any effect of the metal on the ^{23}Na NMR should be readily observable. We measured the ^{23}Na lineshape and found a single resonance at a frequency typical of sodium in ionic compounds. The ^{23}Na resonance shows no indication of a Knight shift. A signal calibration indicates that the observed ^{23}Na signal accounts for all the sodium in the sample. The ^{23}Na spin lattice relaxation varies with temperature as $1/T^2$ suggesting relaxation by quadrupole mechanisms. On the other hand, CO on Pt has a $\sim$130 ppm Knight shift and spin lattice relaxation determined by Ansermet to vary as $1/T$. Both of these characteristics of the CO are attributed to mixing of its molecular orbitals with the Pt conduction band, and their absence for the Na in our samples suggests that the Na interacts with the Pt to a lesser degree than does adsorbed CO.

By performing ^{23}Na – ^{13}C double resonance we found that the sodium coverage on the platinum is at least 0.17 (about half a monolayer) and that the density of the Na's CO neighbors is about that of a c(4×2) pattern on Pt(111). However, despite the presence of a relatively large amount of sodium on the surface, the normalized CO signal for the sample is nearly the same as that of the sample without sodium, indicating the presence of an equal amount of adsorbed CO in the two samples. One could not have this much sodium and CO on the platinum without their being closer together than indicated by SEDOR if the sodium were dispersed as individual sodium atoms or ions.

It seems reasonable that the sodium would be present as Na_2O clusters with sizes approaching molecular dimensions. This is consistent with the result of Andersson et al. who found that Na layers on Ni(100) form Na_2O layers when exposed to O_2 [38]. Although the samples are cleaned and then reduced with H_2 flow at 573 K, the alkali metals remain as oxides. Ertl has determined that when ammonia synthesis catalysts consisting of a mixture of Fe_3O_4 and K_2O are reduced with H_2 flow at about 625 K, the iron oxide is reduced to metallic iron while the potassium remains as an oxide [39].

We measured the ^{13}C lineshape and spin–lattice relaxation for CO on clean platinum and for CO with Na, K, Rb, and Cs on platinum. The presence of the alkali metal has only a small effect on the properties of adsorbed CO. The ^{13}C line for CO is narrowed and shifted to slightly higher frequency while the spin–lattice relaxation is slowed. For CO with Rb, for which the effect of the alkali metal is greatest, the magnitude of the change in the properties of the CO is only about 10–15%. The limited effect of the alkali metal on the NMR properties of CO is consistent with the results of Bajusz et al. in their work on CO methanation on K promoted Pt/SiO_2 catalysts [40]. They studied K/Pt ratios of 0.1 and 0.2 in two different temperature regions and found that in only one case did the presence of the K result in an increase in the rate of CO methanation.

Our results do not support any of the proposed models for alkali metal–adsorbate interaction. A rehybridization of the CO like that proposed by Weimer should produce big changes in the CO chemical and Knight shifts. Unless the changes cancel one another, there is no evidence for such an interaction. Likewise, formation of alkali metal – CO complexes should cause a change in the CO chemical shift. In Heskett's proposed direct interaction between K and CO, a potassium ion is neutralized by charge transfer from CO. Our Na lineshape measurement, however, indicates that the alkali metal in our samples is ionic in character. The fact that our results do not show the big effects predicted by interactions proposed as a result of high vacuum studies is not at all surprising. In our samples, prepared in a manner similar to real catalysts, the alkali metal exists in an ionic compound, most likely an oxide. Its single valence electron is tied up in an ionic bond. In contrast to this, in high vacuum studies, alkali metals are deposited in elemental form in an oxygen free environment. The alkali metal valence electron is free to be donated to the surface, leaving behind the alkali metal ion required for complex formation or for Heskett's direct interaction.

Acknowledgements

This work was supported by the DOE Division of Materials Research under Grant No. DEFG02-91ER45439.

References

[1] W.B. Innes, Catalysis , vol. 1, P.H. Emmett (Ed.), Reinhold, New York, 1954, pp. 245–314.
[2] G. Ertl, Catal. Rev. -Sci. Eng. 21 (1980) 201.
[3] S.D. Spencer, G.A. Somorjai, Rep. Prog. Phys. 46 (1983) 1.
[4] H.P. Bonzel, Surf. Sci. Rep. 8 (1987) 43 .
[5] H.P. Bonzel, J. Vac. Sci. Tech. A 2 (1984) 866 .
[6] R.W. Gurney, Phys. Rev. 47 (1935) 479 .
[7] P. Soukiassian, R. Riwan, J. Lecante, E. Wimmer, S.R. Chubb, A.J. Freeman, Phys. Rev. B 31 (1985) 4911 .
[8] G.P. Lopinski, P.J. Estrup, Bul. Am. Phys. Soc. 36(3) (1991) 854 .
[9] H. Ishida, Phys. Rev. B 38 (1988) 8006.
[10] J. Lee, J. Arias, C.P. Hanrahan, R.M. Martin, H. Metiu, J. Chem. Phys. 82(1) (1985) 485.
[11] J.E. Crowell, G.A. Somorjai, Appl. Surf. Sci 19 (1984) 73.
[12] L.J. Whitman, W. Ho, J. Chem. Phys. 83 (1985) 4808 .
[13] J.C. Bertolini, P. Delechere, J. Massardier, Surf. Sci. 160 (1985) 531.
[14] H.S. Luftman, Y.M. Sun, J.M. White, Appl. Surf. Sci. 19 (1984) 59.
[15] F.M. Hoffman, R.A. dePaola, Phys. Rev. Lett. 52(1984) 1697.
[16] D.A. Wesner, G. Pirug, F.P. Coenen, H.P. Bonzel, Surf. Sci. 178 (1986) 608.
[17] D. Heskett, I. Strathy, E.W. Plummer, R.A. dePaola, Phys. Rev. B 32 (1985) 6222.
[18] W. Wurth, C. Schneider, E. Umbach, D. Menzel, Phys. Rev. B 34 (1986) 1336.
[19] J.J. Weimer, W. Wurth, E. Hudeczek, E. Umbach, J. Vac. Sci. Tech. A 4 (1986) 1347.
[20] J.J. Weimer, E. Umbach, D. Menzel, Surf. Sci. 159 (1985) 83.
[21] D. Lackey, M. Surman, S. Jacobs, D. Grider, D.A. King, Surf. Sci. 152/153 (1985) 513.
[22] P.-K. Wang, J.Ph. Ansermet, P.J.S.L. Rudaz, S. Wang, S. Shore, C.P. Slichter, J.H. Sinfelt, Science 234 (1986) 35.
[23] J.P. Ansermet, C.P. Slichter, John H. Sinfelt, Solid state NMR techniques for study of surface phenomenon, Progress NMR Spectrosc. 22, 1990, 401

[24] C. Brevard, D. Granger, Handbook of High Resolution Multinuclear NMR, Wiley, New York, 1981.
[25] R.T. Schumacher, C.P. Slichter, Phys. Rev. 101 (1956) 58.
[26] A.M. Clogston, V. Jaccarino, Y. Yafet, Phys. Rev.134 Phys. Rev. 134 (1964) A650.
[27] H.S. Gutowsky, B.R. McGarvey, J. Chem. Phys. 20 (1952) 1472.
[28] R. Besohn, J. Chem. Phys. 29 (1958) 326.
[29] E. Fukushima, S. Roeder, Experimental Pulse NMR, A Nuts and Bolts Approach, Addison-Wesley, 1981, 110 pp.
[30] J.-Ph. Ansermet, J.C.P. Slichter, J.H. Sinfelt, J. Chem. Phys. 88 (1988) 5963.
[31] J.-Ph. Ansermet, J.P.K. Wang, C.P. Slichter, J.H. Sinfelt, Phys. Rev. B 37 (1988) 1417.
[32] Dale Durand, Ph.D. Thesis, University of Illinois, 1989.
[33] C.P. Slichter, Principles of Magnetic Resonance, 3rd edn., Springer, Berlin, 1990.
[34] H.E. Rhodes, P.K. Wang, H.T. Stokes, C.P. Slichter, J.H. Sinfelt, Phys. Rev. B 26 (1982) 3559.
[35] R.G. Kidd, J. Goodfellow, in: R.K. Harris, B.E. Mann (Eds.), NMR and the Periodic Table, Academic, New York, 1978, p. 251.
[36] S.L. Rudaz, J.-Ph. Ansermet, P.-K. Wang, C.P. Slichter, J.H. Sinfelt, Phys. Rev. Lett. 54 (1985) 71.
[37] D.M. Washecheck, E.J. Wincherer, L.F. Dahl, A. Cerotti, G. Longoni, M. Manassero, M. Sansoni, P. Chini, J. Am. Chem. Soc. 10 (1979) 6110 .
[38] S. Aandersson, J.B. Pendry, P.M. Echenique, Surf. Sci. 65 (1977) 539.
[39] G. Ertl, N. Thiele, Appl. Surf. Sci. 3 (1977) 99.
[40] I.G. Bajusz, D.J. Kwik, J.G. Goodwin, Catal. Lett. 48 (1997) 151.